EXPERIMENTS OF RISER SLUG FLOW USING TOPSIDE MEASUREMENTS: PART I

Heidi Sivertsen * **Sigurd Skogestad** *,[1]

* *Department of Chemical Engineering, Norwegian University of Science and Technology, Trondheim, Norway*

Keywords: Cascade control, unstable, poles, feedback control, controllability analysis

This paper is the first of two papers describing control experiments on different scale slug lab rigs. This first paper describes the study and results from a small-scale lab rig, build to test different riser slug control strategies without the huge costs involved in larger scale experiments. Earlier experiments on this small-scale rig have shown that it is possible to stabilize the flow using a PI-controller with a pressure measurement located upstream the riser base as measurement (Sivertsen and Skogestad (2005)). The aim now was to control the flow using only topside measurements.

A controllability analysis was performed in order to screen the different measurement candidates using a model developed by Storkaas et al. (2003). The analysis showed that it should be possible to control the flow using only topside measurements. The results from this analysis were then used as a background for the experiments performed in the lab.

The experimental results were successful. They showed that it was possible to control the flow far better then predicted from the analysis and the results were in fact comparable with the results obtained when using a pressure measurement upstream the riser (subsea measurement).

1. INTRODUCTION

The behaviour of multiphase flow in pipelines is of great concern in the offshore oil and gas industry, and a lot of time and effort have been spent studying this phenomena. The reason for this is that by doing relatively small changes in operating conditions, it is possible to change the flow behaviour in the pipelines drastically. This has a huge influence on important factors such as productivity, maintenance and safety. Figure 1 shows different flow regimes that can develop in an upward pipeline.

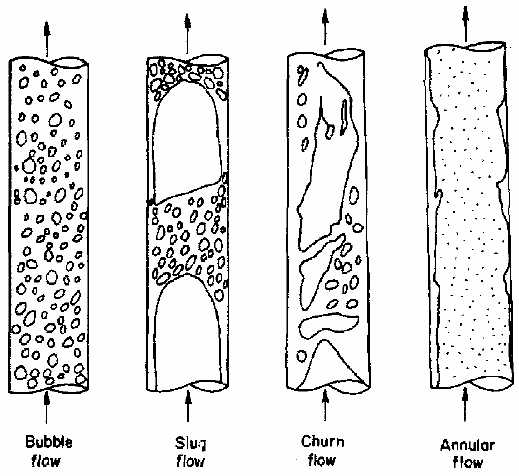

Fig. 1. Vertical horizontal flow map of Taitel et al. (1980)

Some operating conditions lead to an undesirable flow regime that may cause severe problems for the receiving facilities due to varying flow rates and pressure in the system. This usually happens in the end of the life cycle of a well, when flow rates are lower than the system was designed for. The rate and pressure variations are caused by a flow regime called slug flow. It is characterized by alternating bulks of liquid and gas in the pipeline.

[1] Author to whom correspondence should be adressed: skoge@chemeng.ntnu.no

Being able to avoid slug flow in the pipeline is of great economic interest. For this reason it is important to be able to predict the flow regime before production starts, so that the problems can be taken care of as soon as they arise. Traditionally flow maps as the one in Figure 2 have been produced as a tool to predict the flow regime that will develop in a pipeline (Taitel and Dukler (1976), Barnea (1987), Hewitt and Roberts (1969)). These maps show that the flow regime in a pipeline is highly dependent on the incoming superficial flow rates of gas (u_{GS}) and oil (u_{LS}).

Even though the system is designed to avoid such problems in the earlier years of production, the production rate is changed during the production lifetime and problems can arise later on. Note however that these flow maps represent the ”natural” flow regimes, observed when no feedback control is applied.

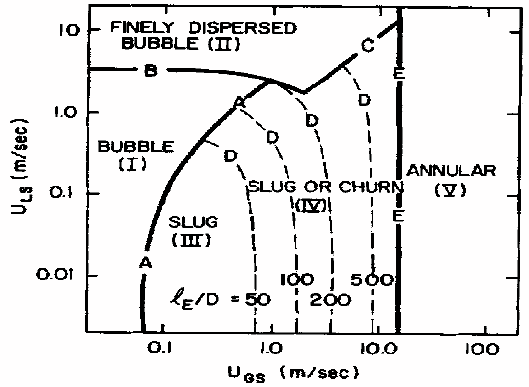

Fig. 2. Flow pattern map for 25 mm diameter vertical tubes, air-water system (Taitel et al. (1980))

There exist different types of slugs, depending on how they are formed. They can be caused by hydrodynamical effects or terrain effects. The slugs can also be formed due to transient effects related to pigging, start-up and blow-down and changes in pressure or flow rates.

Hydrodynamic slugs are formed by liquid waves growing in the pipeline until the height of the waves is sufficient to completely fill the pipe. These slugs can melt together to form even larger slugs and occur over a wide range of flow conditions.

Terrain slugging is caused by low-points in the pipeline topography, causing the liquid to block the gas until the pressure in the compressed gas is large enough to overcome the hydrostatic head of the liquid. A long liquid slug is then pushed in front of the expanding gas upstream.

One example of such a low-point is a subsea line with downwards inclination ending in a vertical riser to a platform. In some cases the entire riser can be filled with liquid until the pressure in the gas is large enough to overcome the hydrostatic pressure of the liquid-filled riser. Under such conditions a cyclic operation (limit cycle) is obtained. It is considered to consist of four steps (Schmidt et al. (1980), Taitel (1986)). These steps are illustrated in Figure 3. Liquid accumulates in the low point of the riser, blocking the gas (1). As more gas and liquid enters the system, the pressure will increase and the riser will be filled with liquid (2). After a while the amount of gas that is blocked will be large enough to blow the liquid out of the riser (3). After the blow-out, a new liquid slug will start to form in the low-point (4).

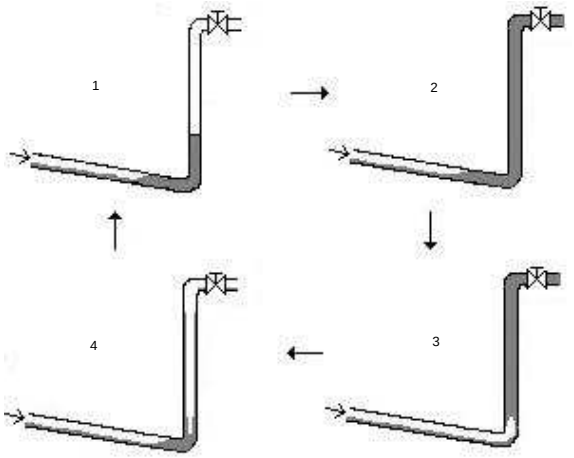

Fig. 3. Illustration of the cyclic behaviour (slug flow) in pipeline-riser systems

Terrain induced slugs can become hundreds of meters long, whereas hydrodynamic slugs are relatively shorter. This is also the reason why terrain slugging is often referred to as severe slugging.

Slug flow has a negative impact on the receiving facilities during offshore oil and gas production due to the large fluctuations in flow rates and pressure. Frequent problems are unwanted flaring and reduced operating capacity. The fluctuating pressure also leads to a lot of strain on other parts of the system, such as valves and bends. The burden on the topside separators and compressors can in some cases become so large that it leads to damages and plant shutdown, representing huge costs for the producing company.

Being able to remove slugging has a great economic potential and this is why lot of work and money has been spent on finding solutions to the problem. It is possible to avoid or handle the slugs by changing the design of the system. Examples of this are; changing the pipeline topology, increasing the size of the separator, adding a slug catcher or installing gas lift. However, the implementation of this new equipment usually costs a lot of money. Another option is changing the operating conditions by choking the topside valve. Also this comes with a drawback; the increased pressure in the pipeline leads to a reduced production rate and can lower the total recovery of the field that is being exploited.

In the last years there have been several studies on active control as a tool to ”stabilize” the flow and thereby avoiding the slug flow regime. Mathematically, the

objective is to stabilize a flow region which otherwise would be unstable. A simple analogue is stabilization of a bicycle which would be unstable without control.

Schmidt et al. (1979) was the first to successfully apply an automatic control system on a pipeline-riser system with a topside choke as actuator. Hedne and Linga (1990) showed that it was possible to control the flow using a PI controller and pressure sensors measuring the pressure difference over the riser. Lately different control strategies have also been implemented on production systems offshore with great success (Hollenberg et al. (1995), Courbot (1996), Havre et al. (2000), Skofteland and Godhavn (2003)). Active control changes the boundaries of the flow map presented in Figure 2, so that it is possible to avoid the slug flow regime in an area where slug flow is predicted. This way it is possible to operate with the same average flow rates as before, but without the huge oscillations in flow rates and pressure.

The advantages with using active control are large; it is much cheaper than implementing new equipment and it also removes the slug flow all together thereby removing the strain on the system. This way a lot of money can also be saved on maintenance. Also, it is possible to produce with larger flow rates than what would be possible by manually choking the topside valve.

Subsea measurements are usually included in the control structures that have been reported in the literature so far. Pressure measurements at the bottom of the riser or further upstream are examples of such measurements. When dealing with riser slugging, subsea measurements have proved to effectively stabilize the flow. When no subsea measurements are available, we will see that the task gets far more challenging.

Since subsea measurements are less reliable and much more costly to implement and maintane than measurements located topside, it is interesting to see if it is possible to control the flow using only topside measurements. Is it possible to combine topside measurements in a way that improve the performance? And are the results comparable to the results obtained when using a controller based on subsea measurements?

Earlier studies on using only topside measurements are found in Godhavn et al. (2005) where experiments where performed on a larger rig and the flow was controlled using combinations of pressure and density measurements. Similar experiments as the ones described in this paper was later performed an a medium-salve lab rig to inestigate the effect the scale of the lab rig has on the quality of the controllers. These experiments are described in Sivertsen et al. (2008).

2. CASE DESCRIPTION

2.1 Experimental setup

To test different control configurations, a small-scale two-phase flow loop with a pipeline-riser arrangement was build at the Department of Chemical Engineering at NTNU, Trondheim (Bårdsen (2003)). The flow consists of water and air, mixed together at the inlet of the system. Both the pipeline and the riser was made of a 20mm diameter transparent rubber hose, which makes it easy to change the shape of the pipeline system. A schematic diagram of the test facilities is shown in Figure 4.

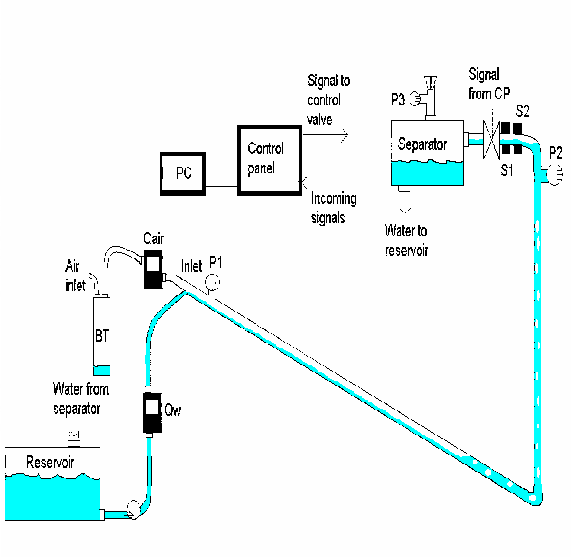

Fig. 4. Experimental setup

From the inlet, which is the mixing point for the air and water, the flow is transported trough a 3m long curved pipeline to the low-point at the bottom of the riser. Depending on different conditions such as water and air flow rates, slug flow may occur. At the top of the riser there is an acryl tank which serves as a separator, leading the water to a reservoir while the air is let out through an open hole in the top. The separator is thus holding atmospheric pressure.

From the reservoir the water is pumped back into the system through the mixing point using a Grundfos UPS 25-120 180 pump with a lifting capacity of 12m. It is possible to adjust the power of the pump, thereby changing the pressure dependency of the inlet flow rate of the water. The pressure dependency during the experiments are discussed in Section 2.3, where periodic disturbances in the inlet flow rate of gas from the air supply system are also described.

For slugging to appear there must be enough air in the system to blow the water out of the 2.7m long riser. This requires a certain amount of volume, which is accounted for by a 15 l acryl buffer tank (BT) between the air supply and the inlet. The volume of the gas can be changed by partially filling this tank with water.

The inlet flow rates of gas (Q_{air}) and water (Q_w) determines whether we will have slug flow in open loop operation or not. The gas flow rate is measured at the inlet using a 2-10 l/min mass flow sensor from Cole-Parmer. The water flow rate was measured using a 2-60 l/min flow transmitter from Gemü. Typically inlet flow rates during an experiment are 5 l/min both for the gas and water.

Pressure sensors MPX5100DP from Motorola are located at the inlet (P_1) and topside (P_2). They measure the pressure difference between the atmospheric pressure and the pipeline pressure in the range 0-1 bar. Typically average values for the pressure during the experiments are approximately 0.2 barg at the inlet and 0.05 barg just upstream the topside control valve.

Two fiber optic sensors (S_1, S_2) from Omron are placed just upstream the control valve in order to measure the water content in the pipeline. Water in the pipeline will attenuate the laser beam and weaken the signal send to the control panel. The measurements from the fiber optic slug sensors needed some filtering because of spikes caused by reflections of the laser beam on the water/air interface (Figure 5). When correctly calibrated, the fiber optic sensors give a signal proportional to the amount of water the laser beam travels through in the pipeline and can be used to calculate the density ρ in the pipeline.

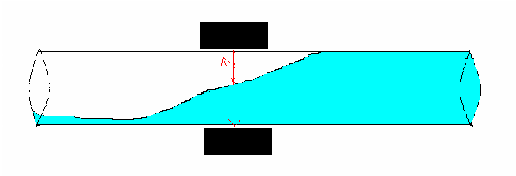

Fig. 5. Reflection of light on water surface

A pneumatic operated Gemü 554 angle seat globe valve with 20 mm inner diameter is installed at the top of the riser. A signal from the control panel sets the choke opening percentage of the valve. The valve responds well within a second to the incoming signal.

The control panel, consisting of Fieldpoint modules from National Instruments, converts the analog signals from the sensors into digital signals. The digital signals are then sent to a computer where they are continuously displayed and treated using Labview software. Depending on the control configuration, some of the measurements are used by the controller to set the choke opening for the control valve.

2.2 Labview software

Labview from National Instruments was chosen as tool for acquiring, storing, displaying and analyzing the data from the different sensors. Also the valve opening of the topside valve was set from this program.

The controllers was made using Labview PID controllers with features like integrator anti-windup and bumpless controller output for PID gain changes.

Also Labviews PID Control Input Filter has been used to filter the noisy fiber optic signals. This is a fifth-order low-pass FIR (Finite Impulse Response) filter and the filter cut-off frequency is designed to be 1/10 of the sample frequency of the input value.

2.3 Disturbances

Two of the largest sources of disturbances during the experiments were the variations in the air and water inlet flow rates. The left plots in Figure 6 shows how the air inlet rate Q_a is fluctuating with a period of approximately 200s between 5.5 and 5.9 l/min when the valve is 10% open and the flow is stable. These 200s fluctuations are caused by the on-off controller used for the pressurized air facility at the laboratory. The fluctuations in water rate Q_w are however quite small for this valve opening.

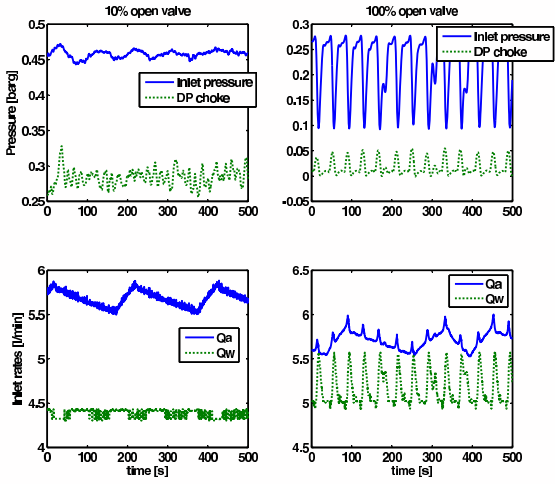

Fig. 6. Disturbances in the inlet water flow rate (Qw) and air inlet rate (Qa)

When the topside valve is fully open and the inlet pressure (P_1) starts to oscillate due to slug flow in the pipeline, larger fluctuations in the water flow was observed. The capacity of the water pump is pressure dependent, and oscillations in the inlet pressure causes the water rate to fluctuate between approximately 4.9 and 5.6 l/min as is seen from the right plots in Figure 6. The pressure oscillations also lead to oscillations in the air inlet flow rate, which come in addition to the 200s periodic fluctuations.

3. CONTROLLABILITY ANALYSIS AND SIMULATIONS

In order to have a starting point for the lab experiments an analysis of the system has been performed.

The analysis reveals some of the control limitations that can be expected using different measurements for control. Closed-loop simulations using these measurements are also performed.

3.1 Theoretical background

Given the feedback control structure shown in Figure 7 the measured output y is found by

$$y = G(s)u + G_d(s)d \tag{1}$$

Here u is the manipulated input, d is the disturbance to the system and n is measurement noise. G and G_d are the plant and disturbance models.

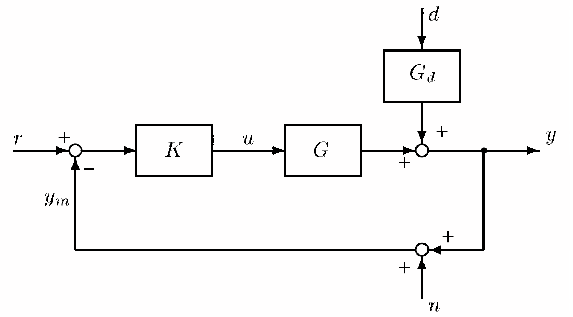

Fig. 7. One degree-of-freedom negative feedback control structure (Skogestad and Postlethwaite (1996))

The location of RHP (Right Half Plane) poles and zeros in $G(s)$ impose bounds on the bandwidth of the system. These bounds can render it impossible to control the system when the RHP-poles and -zeros are located close to each other.

Skogestad and Postlethwaite (1996) shows that a pair of pure complex RHP-poles places a lower bound on the bandwidth of the closed loop system:

$$w_c > 1.15|p| \tag{2}$$

whereas a real RHP zeros imposes an *upper* bound

$$w_c < |z|/2 \tag{3}$$

For an imaginary RHP-zero the bound is

$$w_c < 0.86|z| \tag{4}$$

When comparing Equation (2) with (3) and (4) it is easy to see that if the RHP-zeros and -poles are located close to each other, bandwidth problems can occur.

The closed-loop system also can be expressed as

$$y = Tr + SG_d d - Tn \tag{5}$$

where $T = (I+L)^{-1}L$, $S = (I+L)^{-1}$ and $L = GK$. L is the loop transfer function, whereas S is called the classical sensitivity function and gives the sensitivy reduction introduced by the feedback loop. The input signal is

$$u = KSr - KSG_d d - KSn \tag{6}$$

and the control error $e = y - r$ is

$$e = -Sr + Sg_d d - Tn \tag{7}$$

From these equations it is obvious that the magnitude for transfer functions S, T, SG, KS, KSG_d and SG_d give valuable information about the effect u, d and n have on the system. In order to keep the input usage u and control error e small, these closed-loop transfer functions also need to be small. There are however some limitations for how small the peak values of these transfer functions can be. The locations of the RHP-zeros and -poles influence these bounds significantly.

Minimum peaks on S and T

Skogestad and Postlethwaite (1996) shows that for each RHP-zero z of $G(s)$ the sensitivity function must satisfy

$$||S||_\infty \geq \prod_{i=1}^{N_p} \frac{|z + p_i|}{|z - p_i|} \tag{8}$$

for closed-loop stability. Here $||S||_\infty$ denotes the maximum value of S of the frequency response. This bound is tight for the case with a single RHP-zero and no time delay. Chen (2000) shows that the same bound is tight for T.

Minimum peaks on SG and SG_d

The transfer function SG is required to be small for robustness against pole uncertainty. Similar, SG_d needs to be small in order to reduce the effect of the input disturbances on the control error signal e. In Skogestad and Postlethwaite (1996) the following bounds are found for SG and SG_d

$$||SG||_\infty \geq |G_{ms}(z)| \prod_{i=1}^{N_p} \frac{|z + p_i|}{|z - p_i|} \tag{9}$$

$$||SG_d||_\infty \geq |G_{d,ms}(z)| \prod_{i=1}^{N_p} \frac{|z + p_i|}{|z - p_i|} \tag{10}$$

These bounds are valid for each RHP-zero of the system. Here G_{ms} and $G_{d,ms}$ are the "minimum, stable version" of G and G_d with RHP poles and zeros mirrored into the LHP.

Minimum peaks on KS and KSG_d

The peak on the transfer function KS needs to be small to avoid large input signals in response to noise and disturbances, which could result in saturation. Havre and Skogestad (2002) derives the following bound on KS

$$||KS||_\infty \geq |G_s^{-1}(p)| \tag{11}$$

which is tight for plants with a single real RHP-pole p. Havre and Skogestad (2002) also finds

$$||KSG_d||_\infty \geq |G_s^{-1}(p)G_{d,ms}(p)| \tag{12}$$

When analyzing a plant, all of the closed-loop transfer functions should be considered.

3.2 Modelling

Storkaas et al. (2003) have developed a simplified model to describe the behavior of pipeline-riser slugging. One of the advantages of the model is that it is well suited for controller design and analysis. It consists of three states; the holdup of gas in the feed section (m_{G1}), the holdup of gas in the riser (m_{G2}), and the holdup of liquid (m_L). The model is illustrated by Figure 8.

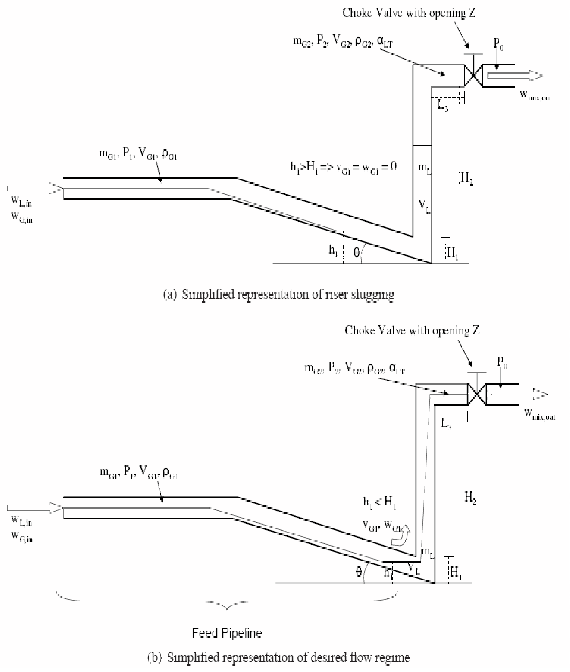

(a) Simplified representation of riser slugging

(b) Simplified representation of desired flow regime

Fig. 8. Storkaas' pipeline-riser slug model (Storkaas et al. (2003))

Using this model we are able to predict the variation of system properties such as pressures, densities and phase fractions and analyze the system around desired operation points.

After entering the geometrical and flow data for the lab rig, the model was tuned as described in Storkaas et al. (2003) to fit the open loop behavior of the lab rig. The model data and tuning parameters are presented in Table 1.

A bifurcation diagram of the system is plotted in Figure 9. It was found by open-loop simulations at different valve openings and gives information about the valve opening for which the system goes unstable. Also the amplitude of the pressure oscillations for the inlet and topside pressure (P_1 and P_2) at each valve opening can be seen from the plot.

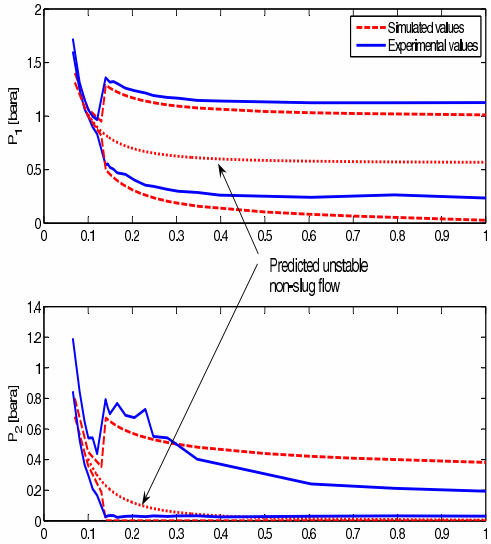

Fig. 9. Bifurcation plot showing the open loop behavior of the system

The upper line in the bifurcation plots shows the maximum pressure at a particular valve opening and the lower line shows the minimum pressure. The two lines meet at around 16% valve opening. This is the point with the highest valve opening which gives stable operation when no control is applied for this particular system. When Storkaas' model is properly tuned, the bifurcation point from the model will match the one from the experimental data. From the bifurcation diagram in Figure 9 it is seen that the tuned model values fit the results from the lab quite well. The dotted line in the middle shows the unstable steady-state solution. This is the desired operating line with closed-loop operation.

Figure 10 shows some of the simulations performed in order to find the bifurcation diagram. The plots show that the frequency predicted by the model is approximately 50% higher than the frequency of the slugs in the lab. In Figure 11 a root-locus diagram of the system is plotted. This plot shows how the poles cross into the RHP as the valve opening reaches 16% from below, confirming the bifurcation diagram in Figure 9.

Table 1. Model data parameters

Parameter	Symbol	Value
Inlet flow rate gas $[kg/s]$	$w_{G,in}$	$1.145 * 10^{-4}$
Inlet flow rate water $[kg/s]$	$w_{L,in}$	0.090
Valve opening at bifurctionpoint [-]	z	0.16
Inlet pressure at bifurcationpoint $[barg]$	$P_{1,stasj}$	0.28
Topside pressure at bifurcationpoint $[barg]$	$P_{2,stasj}$	0.125
Separator pressure $[barg]$	P_0	0
Liquid level upstream low point at bifurcationpoint $[m]$	$h_{1,stasj}$	$9.75 * 10^{-3}$
Upstream gas volume $[m^3]$	V_{G1}	$6.1 * 10^{-3}$
Feed pipe inclination $[rad]$	θ	$1 * 10^{-3}$
Riser height $[m]$	H_2	2.7
Length of horizontal top section $[m]$	L_3	0.2
Pipe radius $[m]$	r	0.01
Exponent in friction expression [-]	n	16
Choke valve constant $[m^{-2}]$	K_1	$2.23 * 10^{-4}$
Internal gas flow constant [-]	K_2	0.193
Friction parameter $[s^2/m^2]$	K_3	$3.4 * 10^3$

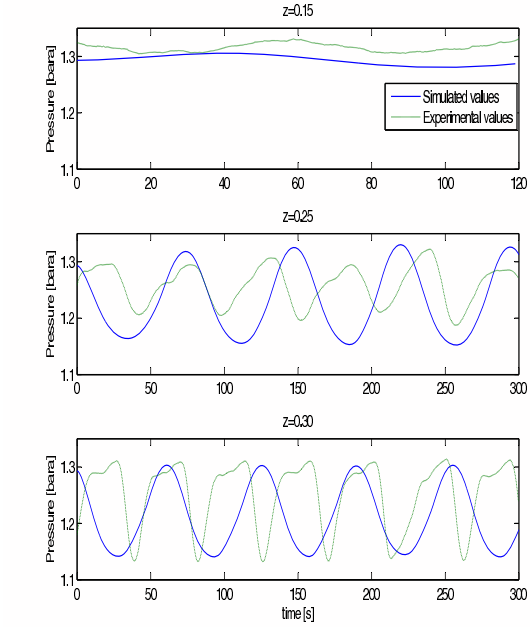

Fig. 10. Open-loop behavior of inlet pressure P_1 for valve openings 15, 25 and 30%

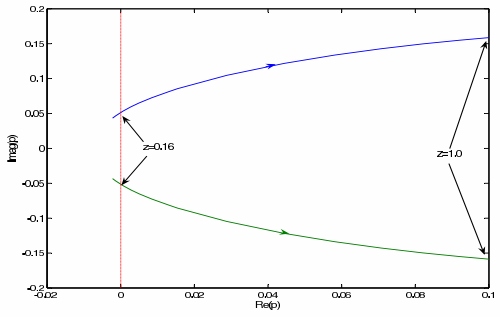

Fig. 11. Root-locus plot showing the trajectories of the RHP open-loop poles when the valve opening varies from 0 (closed) to 1 (fully open)

3.3 Analysis

The model can now be used to explore different measurement alternatives for controlling the flow. The lab rig has four sensors as described in Section 2. There are two pressure sensors; one located at the inlet (P_1) and one topside upstream the control valve (P_2). Also two fiber optic water hold-up measurements are located upstream the control valve. Using these measurements it is possible to estimate the density (ρ) and flow rates (F_Q, F_W) through the control valve. Figure 12 shows the different measurement candidates.

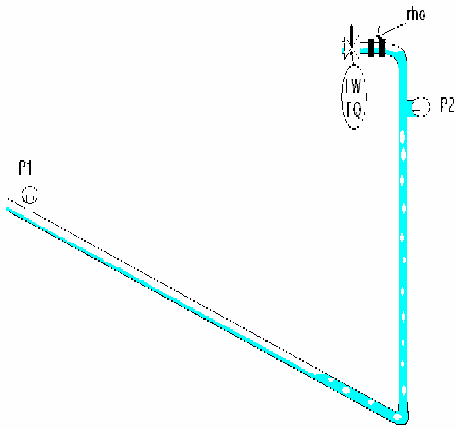

Fig. 12. Measurement candidates for control

In Section 3.1 it was shown how the locations of the RHP poles and zeros had a big influence on the controllability of the system. By scaling the system and calculating the sensitivity peaks it is possible to get a picture of how well a controller, using one of these measurements, can perform.

The only two measurements of the ones considered in this paper which introduces RHP-zeros into the system, are the topside density ρ and pressure P_2. The location of the pair of complex RHP-zeros introduced by P_2 does not cause any concern, as they are much larger and located to the right of the RHP-poles in the complex plane. The real RHP-zero introduced by ρ,

however, seems to be more worrying as it is located to the right of the RHP-poles.

The process model G and disturbance model G_d were found from a linearization of Storkaas' model around two operation points. The model was then scaled as described in Skogestad and Postlethwaite (1996). The process variables were scaled with respect to the largest allowed control error and the disturbances were scaled with the largest variations in the inlet flow rates in the lab. The disturbances were assumed to be frequency independent. The input was scaled with the maximum allowed positive deviation in valve opening since the process gaing is smaller for large valve openings. For measurements $y = [P_1; P_2; \rho; W; Q]$ the scaling matrix is De = diag[0.1 0.05 100 0.01 1*10^{-5} 0.1]. The scaling matrix for the outputs is Dd = diag [1*10^{-5} 1*10^{-2}]. This represents approximately 10% change in the inlet flow rates from the nominal values of 1.145$*10^{-4}$ kg/s (5.73 l/min)for gas and 90$*10^{-}$3 kg/s (5.4 l/min) for water. The input is scaled $Du = 1 - z_{nom}$ where z_{nom} is the nominal valve opening.

Tables 2 and 3 presents the controllability data found. The location of the RHP poles and zeros are presented for valve openings 25 and 30 %, as well as stationary gain and lower bounds on the closed-loop transfer functions described in Section 3.1. The pole location is independent of the input and output (measurement), but the zeros may move. From the bifurcation plot in Figure 9 it is seen that both of these valve openings are inside the unstable area. This can also be seen from the RHP location of the poles.

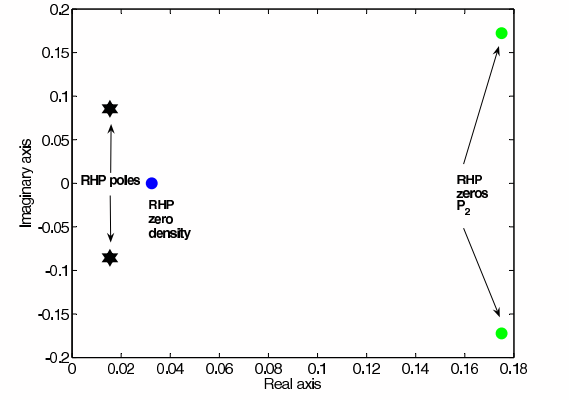

Fig. 13. Plot-zero map for valve opening 30%

The only two measurements of the ones considered in this paper which introduces RHP-zeros into the system, are the topside density ρ and pressure P_2. In Figure 13 the RHP poles and relevant RHP zeros are plotted together. The RHP zeros are in both cases located quite close to the RHP poles, which results in the high peaks especially for sensitivity function SG but also for S. From this we can expect poblems when trying to stabilize the flow using these measurements as single measurements.

The stationary gain found when using the volumetric flow rate F_W is approximately zero, which can cause a lot of problems with steady state control of the system. Also the stationary gain for the plant using density ρ as measurement has a low stationary gain. The model is however based on constant inlet flow rates. The stationary gain for F_W predicted by the model is 0, which means that it is not possible to control the steady-state behavior of the system and the system will drift. Usually the inlet rates are pressure dependent, and the zeros for measurements F_Q and F_W would be expected to be located further away from the origin than indicated by Tables 2 and Table 3.

When comparing $|KS|$ and $|KSG_d|$ for the two tables, it is obvious that the peak values for these transfer function increases with valve opening for all the measurement candidates, indicating that controlling around an operating point with a larger valve opening increases the effect disturbances and noise have on the input usage.

Figure 14 and 15 shows the bode plots for the different plant models and disturbance models respectively. The models were found from a linearization of the model around valve opening 25%. For the volumetric flow rate measurement F_W the value of the disturbance model G_dW is higher than plant model GW for low frequencies. For acceptable control we require $|G(jw)| > |Gd(jw)| - 1$ for frequencies where $|G_d| > 1$ (Skogestad and Postlethwaite (1996)). In this case both $|G_dW|$ and $|G_W|$ is close to zero, which means problems can occur for this measurement.

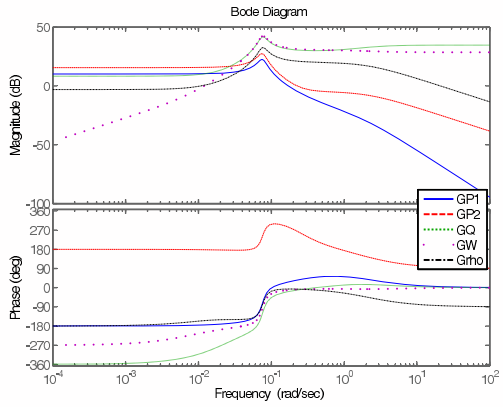

Fig. 14. Bode plots for the plant models using different measurements

3.4 Simulations

Closed-loop simulations were performed in order to investigate the effect of the limitations found in the analysis. The measurements were used as single measurements in a feedback loop with a PI-controller. Figure 16 shows this control structure using the inlet pressure P_1 as measurement.

Table 2. Control limitation data for valve opening 25%. Unstable poles at $p = 0.010 \pm 0.075i$.

Measurement	RHP zeros	Stationary gain	Minimum bounds				
		$\|G(0)\|$	$\|S\|$	$\|SG\|$	$\|KS\|$	$\|SG_d\|$	$\|KSG_d\|$
$P_1[bar]$	-	3.20	1.00	0.00	0.14	0.00	0.055
$P_2[bar]$	0.18±0.17i	5.97	1.13	1.59	0.091	0.085	0.055
$\rho[kg/m^3]$	0.032	0.70	1.20	4.62	0.048	0.31	0.056
$F_W[kg/s]$	-	0.00	1.00	0.00	0.015	1.00	0.055
$F_Q[m^3/s]$	-	2.59	1.00	0.00	0.015	0.00	0.055

Table 3. Control limitation data for valve opening 30%. Unstable poles at $p = 0.015 \pm 0.086i$

Measurement	RHP zeros	Stationary gain	Minimum bounds				
		$\|G(0)\|$	$\|S\|$	$\|SG\|$	$\|KS\|$	$\|SG_d\|$	$\|KSG_d\|$
$P_1[bar]$	-	1.85	1.00	0.00	0.34	0.00	0.086
$P_2[bar]$	0.18±0.17i	3.44	1.22	1.25	0.23	0.085	0.079
$\rho[kg/m^3]$	0.032	0.41	1.26	2.86	0.091	0.31	0.081
$F_W[kg/s]$	-	0.00	1.00	0.00	0.028	1.00	0.079
$F_Q[m^3/s]$	-	1.53	1.00	0.00	0.028	0.00	0.079

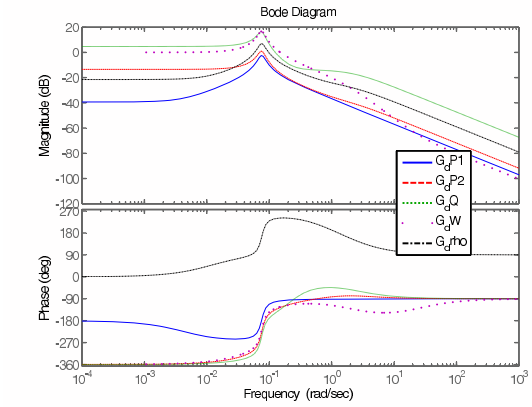

Fig. 15. Bode plots for the disturbance models using different measurements

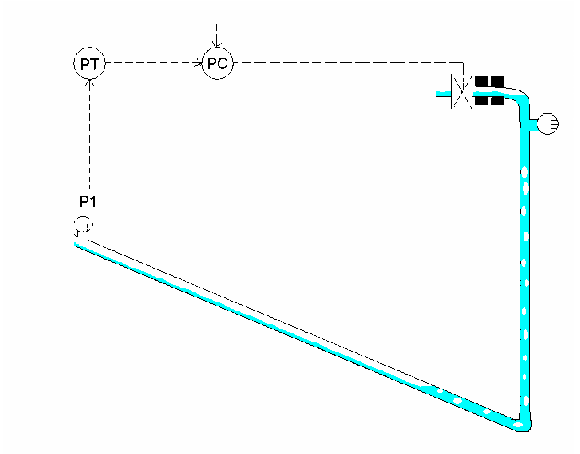

Fig. 16. Feedback control using PI controller with inlet pressure P_1 as measurement

Figure 17 compares the results using four different measurement candidates. The disturbances in inlet flow rates for the gas and water, as described in Section 2.3, are also included in these simulations. The only measurement that is not included, is the topside pressure P_2, as the corresponding controller was not able to stabilize the flow.

At first, the controller is turned off and the system is left open-loop with a valve opening of 20% for approximately 5-10 min. From the bifurcation diagram in Figure 9 it was shown that the system goes unstable for valve openings larger than 16%, as expected the pressure and flow rates start to oscillate due to the effects of slug flow.

When the controllers are activated, the control valve starts working as seen from the right plot in Figure 17. The aim of the simulation study is to see how far into the unstable region it is possible to control the flow with satisfactory performance. A larger valve opening gives higher production with a given pressure dependent source.

As expected the measurement giving the best result was inlet pressure P_1. The upper left plot shows how the controller quickly stabilizes at the desired set point. The average valve opening is 25 %, which is far into the unstable region. After about 70 min the set point for the pressure is decreased, and the valve opening is now larger than 30%. Still the performance of the controller is good.

The figure also shows the results from controlling the flow using the topside volumetric flow rate F_Q, mass flow rate F_W and the density ρ. Not surprisingly the density measurements was not very well suited, as was expected from the analysis in Section 3.3. It was possible to control the flow using this measurement, but not at an average valve opening larger than 17-18% which is just inside the unstable area. The benefits of using control is therefore neglisible.

The small oscillations seen in each plot has a period of 200 s and is caused by the periodic oscillations of the inlet air flow rate.

The results using the topside pressure P_2 are not included in the figure. This is because it was not possible to stabilize the flow inside the unstable region using this measurement. Although the analysis suggested otherwise, the disturbances added in the simulations

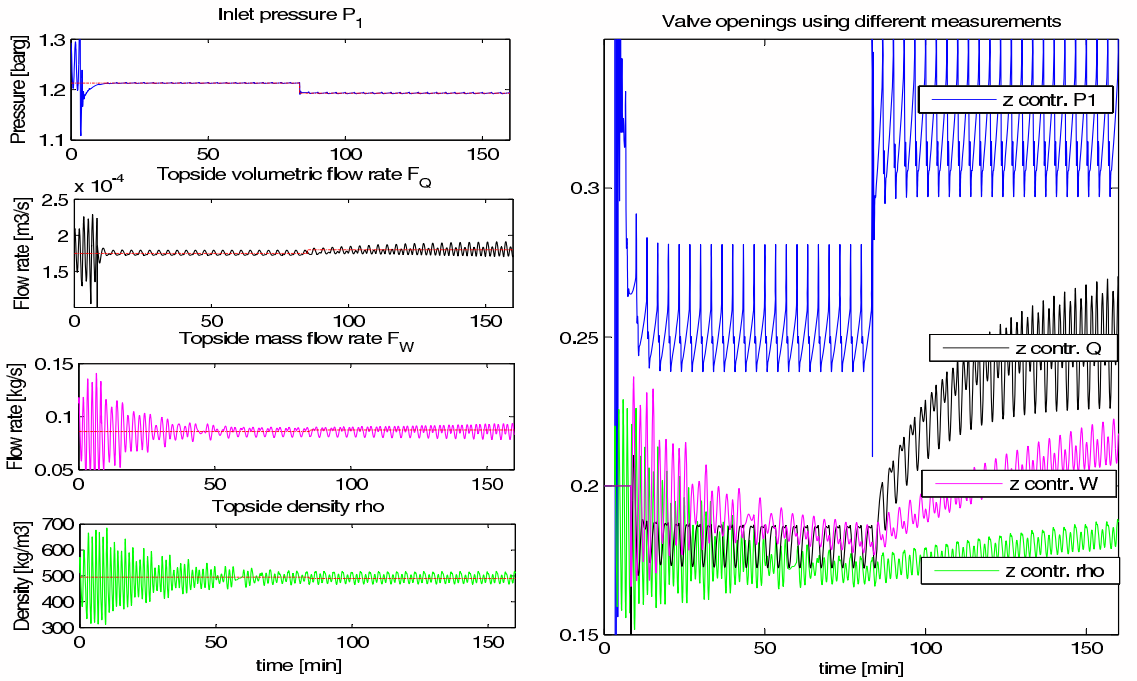

Fig. 17. Controlling the flow using PI controllers

might have had a larger effect on this measurement than on the others.

Sometimes control configurations using combinations of measurements can improve the performance of a controller when compared with controllers using single measurements. This is why cascade controllers using different combinations of the topside measurements have been applied to the system. Figure 18 shows an example of such a control configuration. The inner loop controls the topside density ρ, while the set point for this inner controller is set by an outer loop controlling the valve opening. This way drift due to the low stationary gain for ρ is avoided.

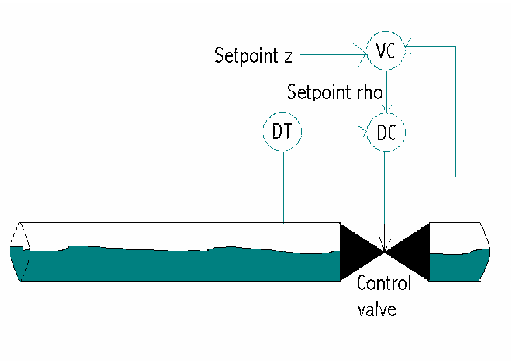

Fig. 18. Cascade controller using measurements density ρ and valve opening z

The results from simulations using this control structure is plotted in Figure 19. The set point for the outer loop controller, controlling the valve opening, is increased from 17% to 18% after approximately 170 min. The flow then quickly becomes unstable, even though the valve opening is just inside the unstable region. The results using this controller is approximately the same as when using the PI controller with density ρ. What is not revealed by Figure 17 however, is whether or not the controller will drift as the simulations is stopped before the controller has stabilized at the desired set point.

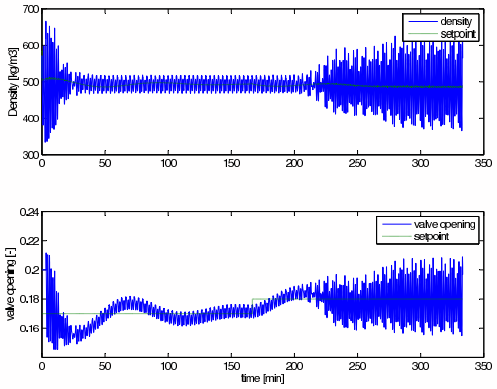

Fig. 19. Simulation results using density ρ and valve opening z as measured variables in a cascade control structure

Using the volumetric flow rate measurement, F_Q, in the inner loop instead would probably give better results as this measurement stabilizes the flow better than the density measurement ρ.

4. EXPERIMENTAL RESULTS

Even though the results from the analysis and simulations suggested that the topside volumetric or mass flow rates F_Q and F_W would be better measurements for control than the topside density ρ, an attempt was

made on controlling the flow using the density as measurement in the inner loop. The density was found using the fiber optic signals.

The reason why flow measurements were not included in the experiments, was because no direct measurements were available. One alternative would be to calculate the flow using a valve equation for two-phase flow and the topside pressure measurement P_2, fiber optic signals S_1 and S_2 and the valve opening z. However, two-phase flow valve equations are quite complicated, and it seemed easier first to use the measurements at hand.

Three different combinations of measurements was tested in a cascade control structure. One of the controllers use the inlet pressure P_1 in the inner loop and the valve opening z in the outer loop. Even though P_1 is not a topside measurement, the results using this controller serve as a basis to compare the other two controllers with.

The other two control structures use the topside density ρ in the inner loop, and had either the valve opening z (Figure 18) or the topside pressure P_2 as a measurement in the outer loop .

Figure 20 shows the experimental results using the three control systems. First the system was left open-loop with a valve opening of 25%. Since this is well inside the unstable area, the pressures and density in the system is oscillating. After about 100s the controllers are turned on, and in both three cases the controllers are able to control the flow. When the controllers are turned off after 500-600s, the flow quickly becomes unstable again. The thick lines indicated the set points for the different controllers.

In plot a) and b) in Figure 20 the valve opening set point for the outer loop was 25% fully open, whereas for the experiment presented in plot c) the set point for the topside pressure P_2 in the outer loop was 0.056. Earlier experiments had shown that this lead to an average valve opening of about 25%.

From the analysis and simulations presented in Section 3, it is expected that the control structure with the inlet pressure P_1 in the inner loop would perform best, as this measurement was by far the best suited for controlling the flow as seen both from simulations and control limitations for each measurement candidate. Also, the density measurement at the laboratory is extremely noisy as the plots in Figure 20 show. Despite all this, looking at the experimental results the differences are less obvious. In fact, using the density ρ as the inner measurement works quite well, contradicting the results from the analysis in Section 3.

The main reason for adding the outer loop is to avoid drift in the inner loop caused by the low steady state gain shown in Tables 2 and 3. Since the results from the experiments using a cascade configuration by far outperform the results from the simulations, it was reason to question the values given by the model. This is why an attempt was made to see whether it was possible to control the flow using the density as *only* measurement for control. Figure 21 shows the results using this PI controller and the density measurement ρ.

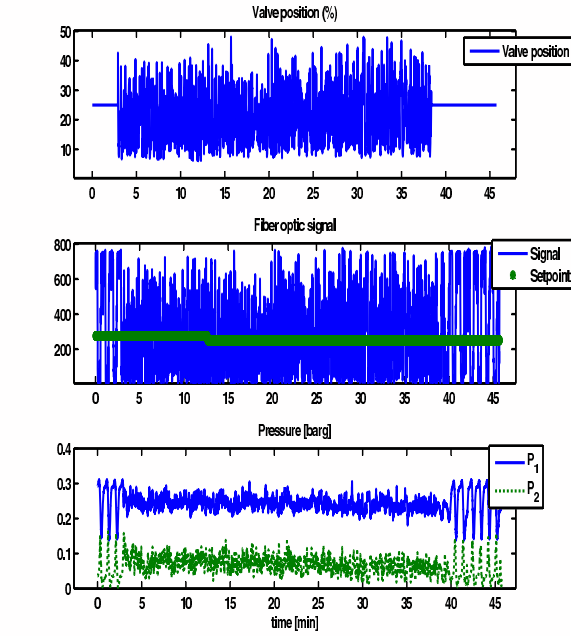

Fig. 21. Experimental results using a PI controller with density ρ as single measurement (no outer loop added)

Also now the controller manages to control the flow. The system does not seem to drift, which means that the steady state gain is not too small for stabilizing the flow in this case.

Controlling the flow at a larger average valve opening led to reduced performance and the flow either became unstable or the controller did not manage to satisfactory keep the measurements at the desired set points (large fluctuations). As the analysis showed, the control task gets harder as the valve opening increases. This is due to the fact that the gain is reduced as the valve opening gets larger. By gradually increasing the average valve opening, either by increasing the setpoint for valve opening in the outer loop or, for case c), reducing the set point for the density, the effect of this increase in valve opening was found. Some results are plotted in the Appendix, where it is seen that the effect of increasing the average valve opening from approximately 24% to 32%using P_1 as measurement leads to increasingly larger fluctuations around the set points. The same experiments were performed for using density ρ as measurement in the inner loop with a) z and b) P_2 in the outer loop. This made the system go unstable as the valve opening was gradually increasing. The average valve opening for which the system goes unstable using these controllers were approximately a) 26% and b) 29%.

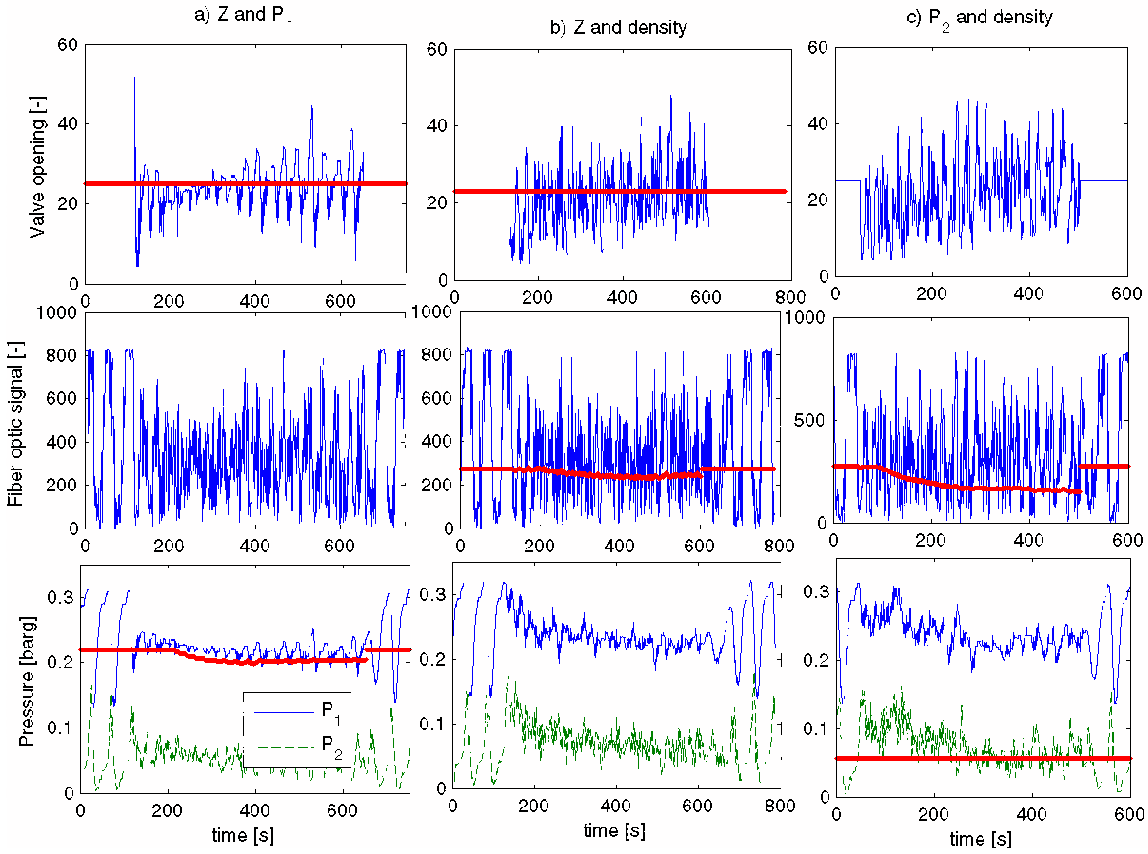

Fig. 20. Results from cascade control experiments at the lab at an approximately valve opening of 25%

5. DISCUSSION

When comparing different controllers, the tuning of the parameters has a high influence on the results. None of the controllers described in this paper have been fine-tuned and the results might be improved further with some more work. This is why the maximum average valve opening for which the controllers stabilize the flow, presented in Section 4, might be increased with proper tuning. However, from the results it seems obvious that all three controllers perform well up to approximately 25% valve opening, and that as the valve opening moves towards an average value of 30% the controller performance decreases for all the controllers.

It is important to note that the model used for the analysis is a very simplified model. It was used merely as a tool to see which problems might occur in the lab, and the underlying reasons for the problems. When comparing the experimental results with analysis and simulations using Storkaas' model prior to the experiments, it was clear that the experimental results were far better than the model predicted when using the density as measurement. On the other hand, the topside pressure P_2 could not be used for stabilization, in agreement with Storkaas' model.

An attempt was made to model the small-scale rig using multiphase simulator OLGA from Scandpower Petroleum Technologies. However, the simulations seemed to fail due to numerical errors, which could be caused by the small-scale nature of the rig.

Even though results using only a PI controller and a single topside density measurement seemed to work very well, without the expected steady state drift, there are other advantages in adding an outer loop. One example of such is that it may be more intuitive to understand what is going on with the plant when adjusting the set point for the valve opening rather than the set point for the topside density.

The experiments have been conducted on a small-scale rig with only 20mm inner diameter pipeline. Whether or not the results can be directly applied to larger test facilities was further investigated in Sivertsen et al. (2008). The results from these experiments showed that similar controllers as the ones described in this paper, also were successful when applied to a medium scale lab rig with a 10m high riser and 7.6 cm diameter pipelines.

6. CONCLUSION

This paper presents results from a small-scale riser laboratory rig where the aim was to control the flow using only topside measurements and thereby avoiding slug flow in the pipeline. The results were good in the sense that it was possible to control the flow with good performance far into the unstable region. In order

to avoid the slug merely by choking the topside valve it would be necessary to operate with a valve opening of 15%, whereas here it was shown that it was possible to control the flow with an average valve opening of 25%, despite very noisy measurements. This makes it possible to produce with a larger production rate and increase the total recovery from the producing oil field.

APPENDIX

Figures showing the behavior when increasing the setpoint, z_s for the outer loop using measurment P_1 in the inner loop:

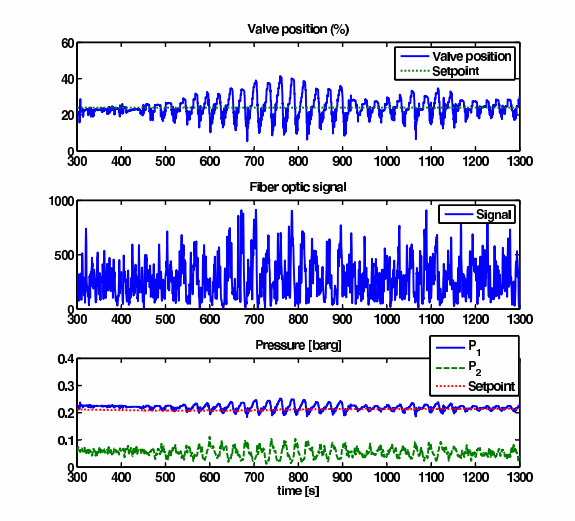

Fig. 22. Control quality when setpoint outer loop is 24%

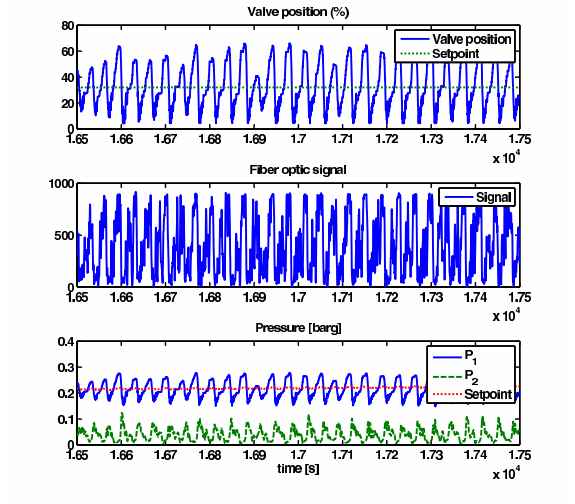

Fig. 23. Control quality when setpoint outer loop is 32%

REFERENCES

I. Bårdsen. Slug regulering i tofase strømning - eksperimentell verifikasjon, November 2003.

D. Barnea. A unified model for predicting flow pattern transitions for the whole range of pipe inclinations. *Int. J. Multiphase Flow*, 13:1–12, 1987.

J. Chen. Logarithmic integrals, interpolation bounds and performance limitations in MIMO feedback systems. *IEEE Transactions on Automatic Control*, AC-45(6):1098–1115, 2000.

A. Courbot. Prevention of severe slugging in the Dunbar 16" multiphase pipeline. *Offshore Technology Conference, May 6-9, Houston, Texas*, 1996.

J.M. Godhavn, M.P. Fard, and P.H. Fuchs. New slug control strategies, tuning rules and experimental results. *Journal of Process Control*, 15(15):547–577, 2005.

K. Havre and S. Skogestad. Achievable performance of multivariable systems with unstable zeros and poles. *International Journal of Control*, 74:1131–1139, 2002.

K. Havre, K. O. Stornes, and H. Stray. Taming slug flow in pipelines. *ABB review*, 4(4):55–63, 2000.

P. Hedne and H. Linga. Supression of terrain slugging with automatic and manual riser choking. *Advances in Gas-Liquid Flows*, pages 453–469, 1990.

G.F. Hewitt and D.N. Roberts. Studies of two-phase flow patterns by simultaneous x-ray and flash photography. Technical report, UKAEA Report AERE M-2159, 1969.

J.F. Hollenberg, S. de Wolf, and W.J. Meiring. A method to supress severe slugging in flow line riser systems. *Oil and Gas Journal (str oppft ogs som Multiphase95)*, 1995.

Z. Schmidt, J.P. Brill, and H. D. Beggs. Choking can eliminate severe pipeline slugging. *Oil & Gas Journal*, (12):230–238, Nov. 12 1979.

Z. Schmidt, J.P. Brill, and H.D. Beggs. Experimental study of severe slugging in a two-phase pipeline-riser system. *Soc. Petrol. Engrs J.*, pages 407–414, 1980. SPE 8306.

H. Sivertsen and S. Skogestad. Anti-slug control experiments on a small scale two-phase loop. *ESCAPE'15, Barcelona, Spain*, 29. Mai- 1. June 2005.

H. Sivertsen, V. Alstad, and S. Skogestad. Experiments of riser slug flow using topside measurements: Part ii. 2008.

G. Skofteland and J.M. Godhavn. Suppression of slugs in multiphase flow lines by active use of topside choke - field experience and experimental results. In *Proceedings of multiphase '03, San Remo, Italy, 11-13 June 2003*, 2003.

S. Skogestad and I. Postlethwaite. *Multivariable feedback control*. John Wiley & sons, 1996.

E. Storkaas, S. Skogestad, and J.M. Godhavn. A low-dimentional model of severe slugging for controller design and analysis. In *Proceedings of multiphase '03, San Remo, Italy, 11-13 June 2003*, 2003.

Y. Taitel. Stability of severe slugging. *Int. J. Multiphase Flow*, 12(2):203–217, 1986.

Y. Taitel and A.E. Dukler. A model for predicting flow regime transitions in horizontal and near-horizontal gas-liquid flow. *AIChE Journal*, 22:47–55, 1976.

Y. Taitel, D. Barnea, and A.E. Dukler. Modeling flow pattern transitions for steady upward gas-liquid flow in vertical tubes. *AIChE Journal*, 26:345–354, 1980.